Supporting Information

Production of formate from CO_2 gas under ambient conditions: towards flow-through enzymes reactors

Mohamed Baccour†, Alexandra Lamotte†§, Kento Sakai‡, Eric Dubreucq§, Ahmad Mehdi†, Kenji Kano‡, Anne Galarneau†, Jullien Drone*†, Nicolas Brun*†

†Institut Charles Gerhardt Montpellier (ICGM), Univ Montpellier, CNRS, ENSCM, Montpellier (France)

‡Division of Applied Life Sciences, Graduate School of Agriculture, Kyoto University, Sakyo, Kyoto (Japan)

§Ingénierie des Agropolymères et Technologies Emergentes, UMR IATE, Univ. Montpellier-SupAgro-INRA-CIRAD, Montpellier (France)

Table of Contents

S1- PtDH production and characterization

The genetic construct encoding of the phosphite dehydrogenase (PtDH) was obtained by courtesy of Prof. H. M. Zhao (University of Illinois) [1] and produced and purified by Rémi Cazelles [2]. In brief, *Escherichia coli* BL21*(DE3) (Life Technologies) was transformed by the plasmid pET15b-PTDH12x and used to overexpress the enzyme as previously described with slight modifications. Homogeneous enzyme preparation was obtained after purification using IMAC Ni^{2+} (HisTrap 1 mL, GE Healthcare) followed by desalting (HiTrap 5 mL, GE Healthcare) with conservation buffer (50 mM MOPS, 10% glycerol, pH 7.25) under standard conditions. Aliquots of the enzyme were stored at −80 °C until use.

Specific activity of PtDH (U$_{PtDH}$)

The specific activity of **PtDH** (U$_{PtDH}$) was determined by monitoring the reduction of NAD cofactor and the production of NADH which absorbs at 340 nm. The evolution of the absorbance is plotted against time (fig. S1).
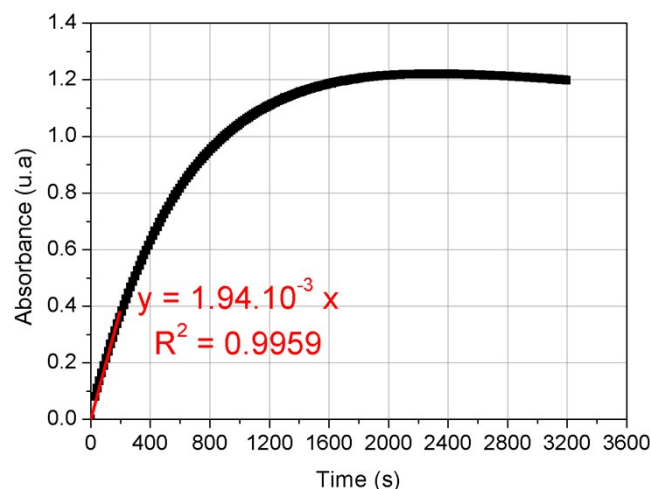

$$y = 1.94.10^{-3} x$$
$$R^2 = 0.9959$$

Figure S1. Absorbance = f (time) of the production of NADH in presence of PtDH at 340 nm plotted against time.

The initial rate is calculated from the slope between 0 and 195 s.

Abs = 0.00194 t

$$V = \frac{Abs}{t} = \frac{\varepsilon.l.C}{t} = \frac{\varepsilon.l.n}{t.V} = \frac{\varepsilon.l.U}{V} = 0.00194 \text{ s}^{-1}$$

$$U_{PtDH} = \frac{v.V}{\varepsilon.l} = 3.743.10^{-2} \text{ µmol NADH}_{produced}/\text{min (for 4 µL of \textbf{PtDH} enzymatic}$$

solution)

The **PtDH** concentration is 7.3 µg/µL. This concentration was determined by Bradford method using bovine serum albumin (BSA) as standard.

$$U_{PtDH} = 1.28.10^{-3} \text{ µmol NADH}_{produced}/\text{min for 1 µg \textbf{PtDH} in initial rate phase.}$$

S2- FoDH production and characterization

S2.1- Commercial *Cb*FoDH

Formate dehydrogenase (Homo-dimer, 80.7 kDa) from Candida boidinii (CbFoDH) was purchased from Sigma-Aldrich.

S2.2- *Ts*FoDH

Formate dehydrogenase from *Thiobacillus sp.* KNK65MA was produced and purified according to the literature [3]. Homogeneous enzyme preparation was obtained after purification using IMAC Ni^{2+} (HisTrap 1 mL, GE Healthcare) followed by desalting (HiTrap 5 mL, GE Healthcare) with conservation buffer (50 mM MOPS, 10% glycerol, pH 7.25) under standard conditions. Aliquots of the enzyme were stored at −80 °C until use.

S2.3- *Me*FoDH1

Formate dehydrogenase from *Methylobacterium extorquens* was provided by Pr. K. Kano (Kyoto University, Japan). *Me*FoDH1 was produced and purified according to the literature [4]. Methylobacterium extorquens AM1 (NCIMB 9133) was purchased from NCIMB (Aberdeen, Scotland, UK). The cells were grown at 28°C in modified Luria broth, which consisted of 1% hipolypepton, 1% yeast extract, 0.5% sodium chloride, 1 µM sodium tungstate and 0.5 µM sodium molybdate. The cells were cultivated in 500 mL Erlenmeyer flasks filled with 150 mL medium. The cells were collected, suspended with 20 mM potassium phosphate buffer (KPB) pH 6.0 and then disrupted two times with a French pressure cell (Otake Works, Japan) at 100 MPa. Centrifugation was performed at 100,000 RPM for 1 h at 4 °C to remove cell debris. The supernatant solution was loaded on a Toyopearl DEAE-650 M column (Tosoh Corporation, Japan) equilibrated with 20 mM KPB pH 6.0. *Me*FoDH1

was eluted with linear gradient of NaCl from 120 mM to 180 mM in the KPB pH 6.0. The sample was collected and applied to a Toyopearl Butyl-650 M column (Tosoh Corporation, Japan) equilibrated with the KPB containing 20% (w/w) ammonium sulfate. The elution of *Me*FoDH1 was carried out under a linear gradient of ammonium sulfate from 12% to 8% in the same KPB pH 6.0. All purification steps were performed at 4°C under aerobic conditions. Protein concentrations were determined with the Pierce® BCA Protein Assay Kit (Thermo Scientific, USA) using bovine serum albumin as a standard. The purities of *Me*FoDH1 were judged by Coomassie brilliant blue R-250 staining of SDS-PAGE. The enzyme is a heterodimer with two units (a1b1) of 107 and 61 kDa, respectively (fig. S2).
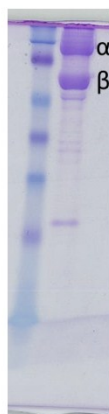

Figure S2. SDS page of *Me*FoDH1.

Specific activity of *Me*FoDH1 (U$_{MeFoDH1}$)

The specific activity of **Me**FoDH1 (U$_{MeFoDH1}$) was determined by oxidizing the reduced form of the NAD cofactor while reducing Na$_2$CO$_3$. This oxidation was monitored by UV absorbance at 340 nm (fig. S3).
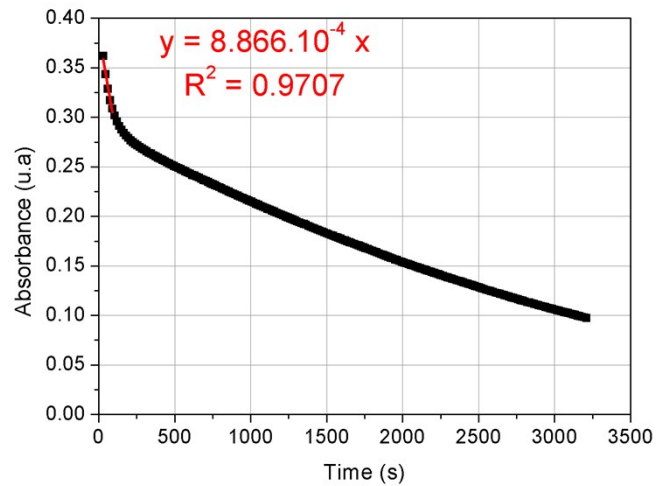
Figure S3. Absorbance = f (time) of the consumption of NADH by *Me*FoDH1 at 340 nm plotted against time.

The initial rate of the consumption of NADH is calculated from the slope between 0 and 90 s.

Abs = $8.86693.10^{-4}$ t

$$V = \frac{Abs}{t} = \frac{\varepsilon.l.C}{t} = \frac{\varepsilon.l.n}{t.V} = \frac{\varepsilon.l.U}{V} = 8.86693.10^{-4} \text{ s}^{-1}$$

$$U = \frac{v.V}{\varepsilon.l} = 0.017 \text{ μmol NAD}^+_{produced}/\text{min (for 4 μL of } \textbf{\textit{Me}FoDH1} \text{ enzymatic solution)}$$

The **_Me_FoDH1** concentration is 15.4 μg.μL^{-1}. This Concentration is determined with Bradford method using BSA as reference.

$U_{\textit{Me}FoDH1}$ = $2.76.10^{-4}$ μmol NAD$^+_{produced}$/min for 1 μg **_Me_FoDH1** in initial rate phase.
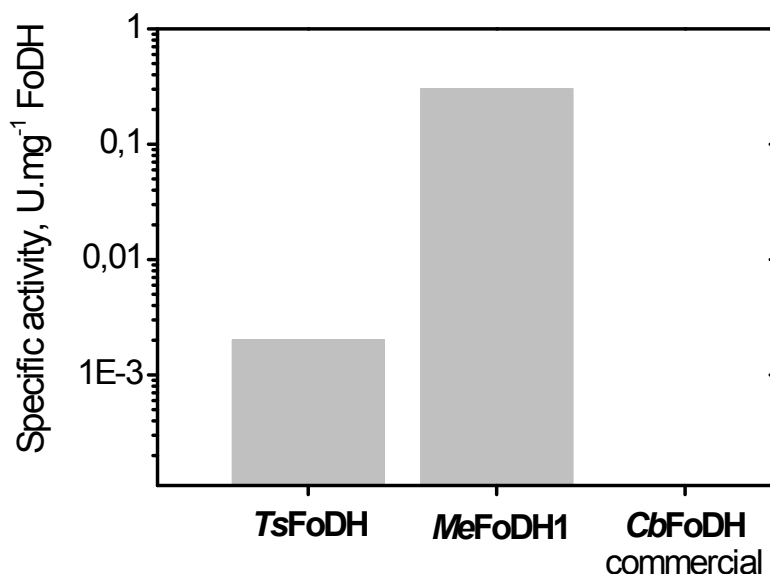
S2.4- Comparison of specific activities

Figure S4. Specific activity of the three formate dehydrogenases employed in this study

S3- Formate monitoring: HPLC analytical procedure

In order to determine the retention time of the different species present in the reaction medium and make sure that it would be possible to measure the concentration of formate, we analyze each ionic species with high performance liquid chromatography. The measurements are done with UV detector at 210 nm. The obtained chromatograms (fig. S5) show that only formic acid has a retention time of 19.97 ± 0.38 min. The bioreduction of CO_2 could be monitored by dosing formic acid produced with ion exchange chromatography.
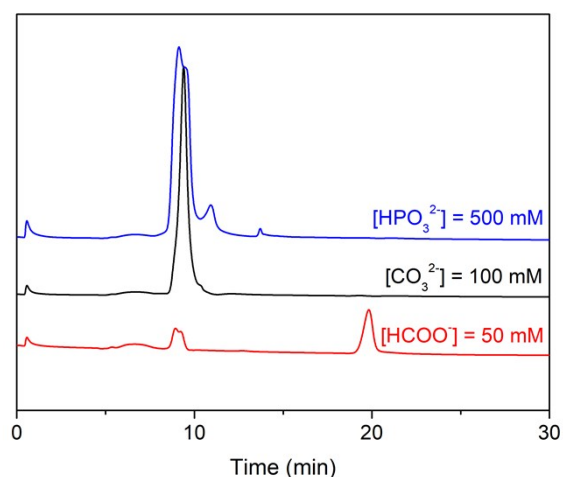
Figure S 5. Chromatograms of three samples: formic acid, carbonate and phosphite buffer.

A standard range with different concentration of formate was prepared: Sodium bicarbonate $[Na_2CO_3]$ = 100 mM, phosphite buffer $[Na_2HPO_3]$ = 500 mM and formic acid $[HCOO^-]$ = 0 ; 1 ; 2 ; 4 ; 8 ; 16 ; 32 ; 64 and 100 mM. This standard was prepared with a concentration of H_2SO_4 equivalent to that of the mobile phase $[H_2SO_4]$ = 2.5 mM.
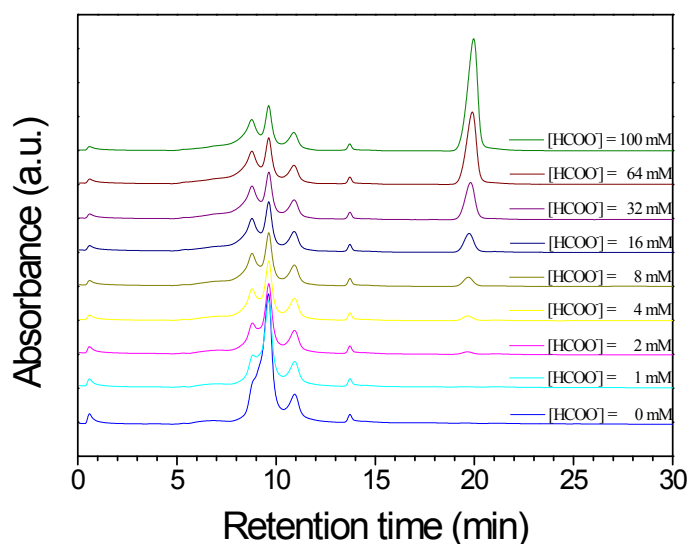

Figure S6. Chromatograms obtained for formate standard range.

The chromatograms show that the intensity and the peak area at the retention time 19.97 ± 0.38 min increase by the increasing of the concentration of formate [HCOO⁻]. A standard range [HCOO⁻] = function (Peak area at t_r = 19.97 ± 0.38 min) was obtained (fig. S7).

Figure contains plot with axes "Peak area (a.u.)" versus "Formate concentration (mM)" with equation:

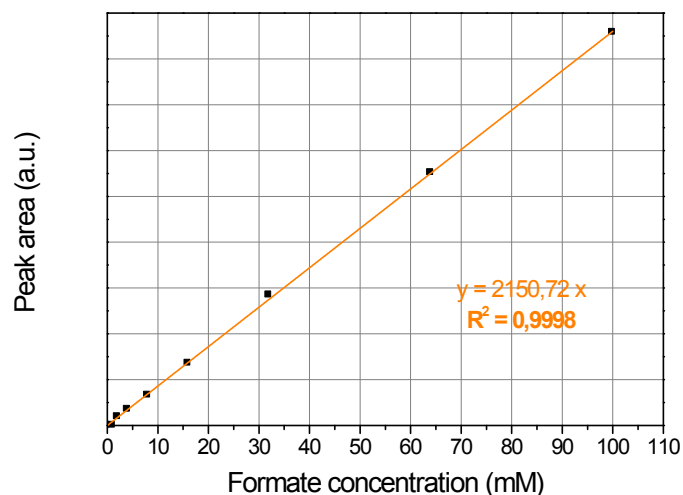$$y = 2150{,}72\ x$$
$$R^2 = 0{,}9998$$

Figure S 7. Peak area at t_r = 19.97 ± 0.38 min as a function of formate concentration

S4- Batch reaction

S4.1- Experimental procedure

The procedure consists on preparing a 2 mL solution "S" which contains [NaHCO$_3$] = 100 mM ; [Na$_2$HPO$_3$] = 500 mM ; and [NAD⁺] = 0.25 mM. (65.81 - 263.24) µg pure PtDH, (61.61 - 246.44) µg pure *Me*FoDH1, and (0 ; 10 ; 20 ; 40 µL) PEGDGE (M$_n$ 500 Da) were added to "S" and the solution was stirred at 500 rpm during 30 min with or without CO$_2$ bubbling as detailed below. All reactions were performed in test tubes with septum caps. The first fraction of 1 mL was recovered after 5 min of stirring and the second fraction was recovered after 30 min of reaction.

S4.2- Influence of CO$_2$ bubbling

The same experiment detailed in S4.1 was done with and without bubbling CO$_2$. CO$_2$ gas (≥ 99.995 %, Air Liquide) was bubbled through a septum cap from a compressed gas cylinder equipped with a manometer and connected to a flowmeter at a constant flow rate of *ca.* 200 mL min⁻¹.
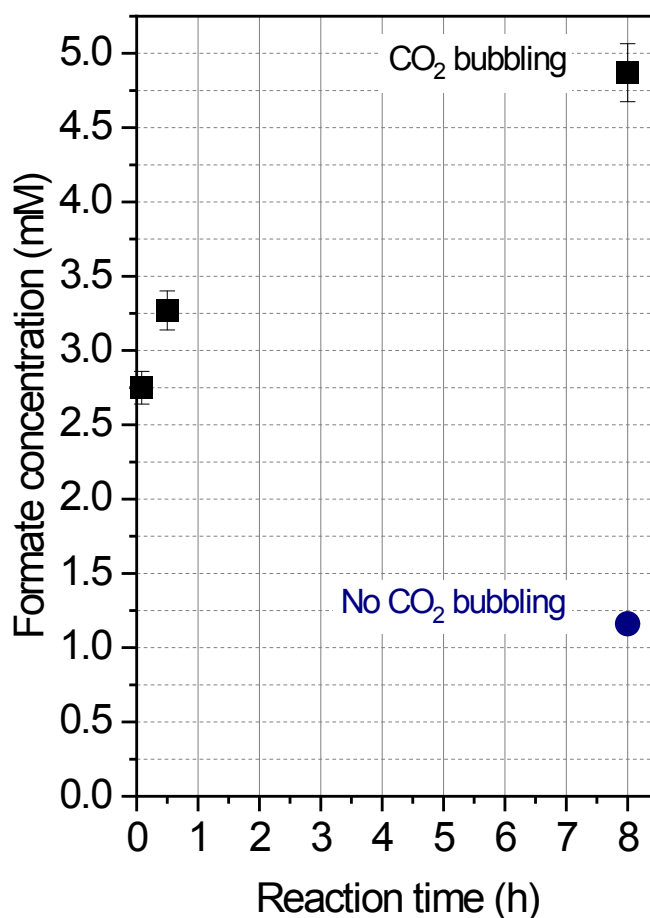
Figure S 8. Formate concentration as a function of time with and without CO_2 bubbling.

S5- Flow through reaction

S5.1- Monoliths preparation and characterization

The first step consists on preparing a silica monolith according to the procedure detailed in the literature.[5] In order to add a carbon replica, the obtained silica monolith with hierarchical porosity has been functionalized with amino groups, keeping the porous structure, to allow a better impregnation of a sucrose solution (carbon precursor).[6]

Amino-functionalization of SiO_2 monolith

The silica monolith was functionalized with 3-(amino propyl) triethoxysilane (APTES) $H_2N(CH_2)_3Si(OC_2H_5)_3$. The functionalization consists on immerging the

silica monolith in a solution of 3.6 mL APTES in 50 mL ethanol. The functionalization was done using a reflux condenser at 80 °C during 18 h.

The obtained amino-functionalized silica monolith was washed with ethanol and dried à 80 °C during 48 h.

Hydrothermal carbonization

0.36 g of amino-functionalized silica monolith SiO_2-NH_2 was immersed into 25 mL of 1.26 M sucrose solution. The impregnation solution and monoliths underwent a treatment into a Teflon inlet inside a stainless steel autoclave at 110 °C during 2 h to force the diffusion of sucrose (carbon precursor) into the mesoporous network. Then the sucrose underwent a hydrothermal carbonization at 180 °C during 16 h. The resulting brown composite SiO_2-hydrochar was washed with water, ethanol and acetone until uncolored wash solution was observed. Then it was dried at room temperature. The composite SiO_2-hydrochar was pyrolyzed as follow: 2 h at 350 °C, 2 h at 550 °C and 2 h at 950 °C with a ramp of 2 °C/min in a tubular oven under argon flow (150 mL.min^{-1}). The SiO_2-carbon composite was obtained.

SiO_2 was removed from the SiO_2-carbon composite by treating it with sodium hydroxide solution (NaOH, 2M) at 100 °C during 24 h to obtain the monolithic carbon replica. The monolithic carbon replica was then washed with water and ethanol and dried at 100°C overnight.
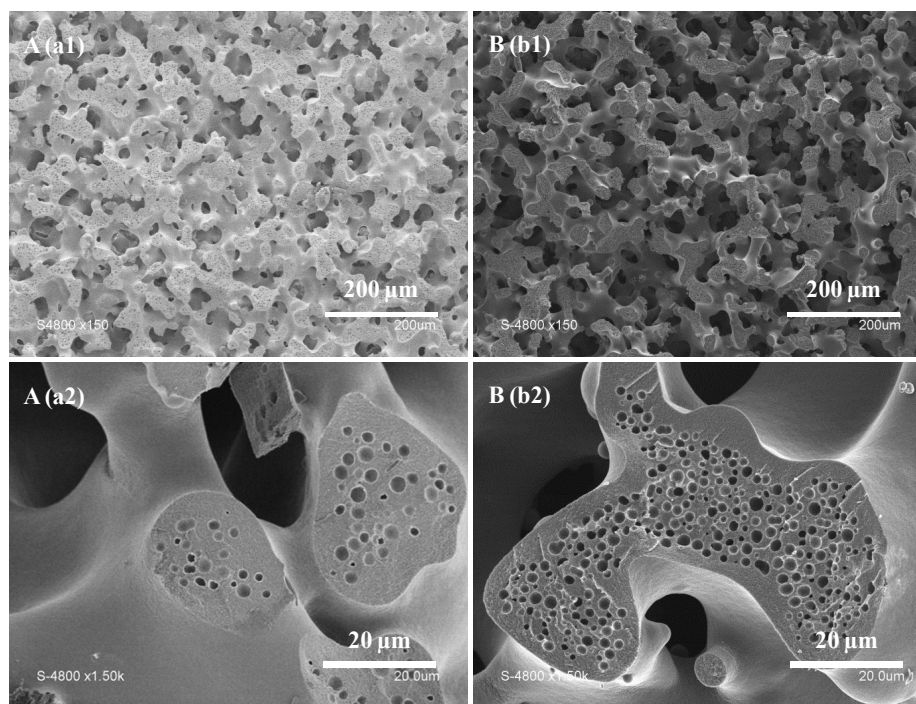
Figure S 9. Scanning electron micrographs of (A) the silica monolithic support and (B) the carbon monolithic support.

Monolith	S_{BET}^{ϕ} (m^2/g)	$V_{macro}^{\S}$ $(cm^3 g^{-1})$	V_{meso}^{ϕ} $(cm^3 g^{-1})$	$V_{micro}^{\ddagger}$ $(cm^3 g^{-1})$	$\varnothing_{macropores}^{\S}$ (μm)	$\varnothing_{mesopores}^{\dagger}$ (nm)
Silica	324	1.9	0.9	--	41 ± 4	20
Carbon replica	1100	2.5	1.9	0.15	35 ± 4	7 & 13

Table S1. Textural properties of the native silica monolith and its carbon replica determined by §Hg porosimetry, $^{\phi}$N$_2$ sorption at 77 K, †BJH method (desorption) and ‡t-plot method.

S5.2- Experimental procedure

The design of the reactor consisted on putting a monolith (55 mg carbon or 85 mg silica; which corresponded to a total pore volume of *c.a.* 0.24 mL for each monolith) between two steel tubes into a heat shrinkable Teflon sheath (FEP AWG 6 from Castello France). The reactor is placed into a tubular oven. The tube is drawn under vacuum then placed under argon flow (150 mL.min^{-1}) in order to preserve the carbon monolith during the thermal treatment. The temperature is fixed at 350 °C with a ramp of 10 °C/min during 10 min.

Once we obtained the reactor, 20 mL of phosphite buffer solution 500 mM, pH 6.4 was circulated through the reactor at a rate of 0.2 mL.min^{-1} allowing its conditioning before the immobilization of enzymes. Subsequently, 0.276 mL of an enzymatic solution, equivalent to the total volume of the reactor, containing 500 mM phosphite buffer pH 6.4, 263.23 µg PtDH, 246.44 µg *Me*FoDH1, 40 µL PEGDGE and 0.25 mM NAD$^+$, is passed through the monolith at a rate of 0.2 mL.min^{-1} in order to fill its porosity. Then the reactor is placed at 4 °C during 24 hours. Enzymes aggregates (*Me*FoDH1 + PtDH) were formed thanks to PEGDGE. In these aggregates NAD cofactor is expected to be trapped. Thereafter, the reactor is washed by circulating 20 mL of phosphite buffer solution 500 mM pH 6.4 at a rate of 0.2 mL.min^{-1}.

A solution containing 500 mM phosphite buffer pH 6.4 and 100 mM NaHCO$_3$, where CO$_2$ was bubbled was passed through the reactor at a rate of 0.2 mL.min^{-1} and 1 mL fractions were recovered every 5 min during 45 min. The fractions were analyzed by HPLC in order to monitor the production of formate.
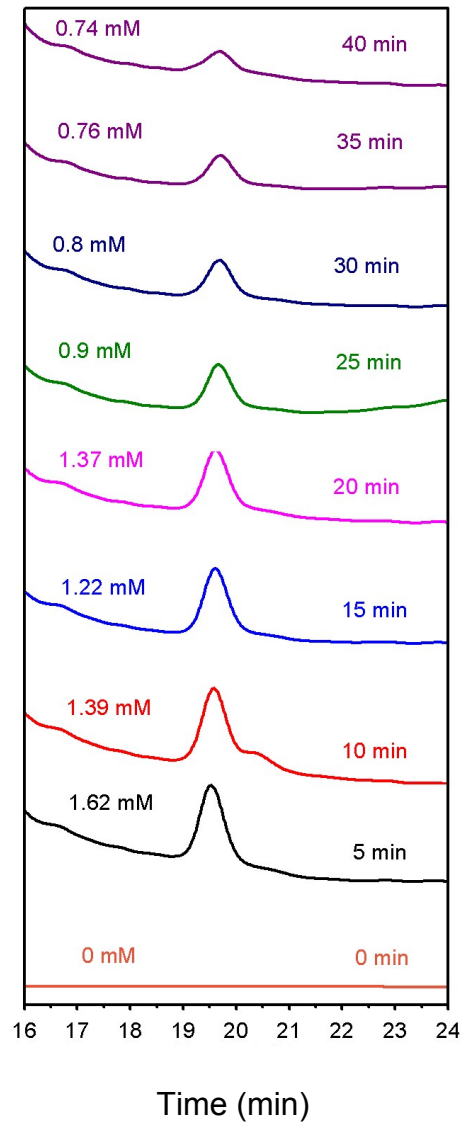
Figure S10. Typical chromatograms obtained for the flow through reactor with carbon monolith

S6- CO_2 adsorption isotherms of monolithic supports at 298 K
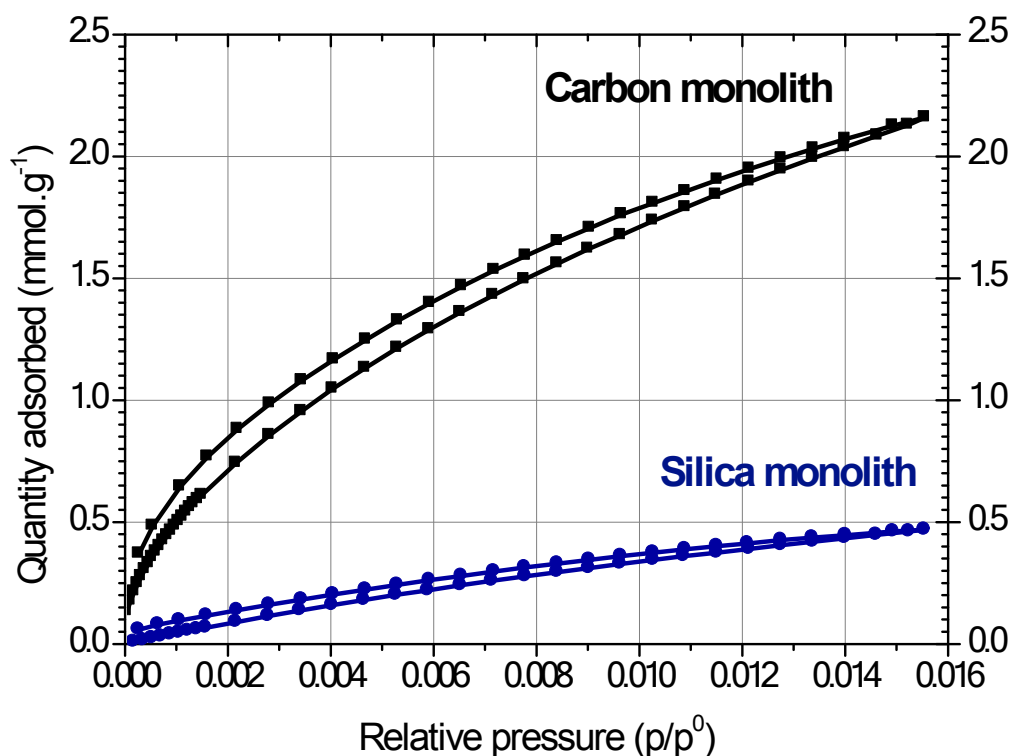
Figure S11. CO_2 adsorption isotherms of monolithic supports performed at 298 K from $p/p^0 = 0$ to $p/p^0 = 0.0156$ (1 atm), using a Micromeritics 3Flex surface characterization analyzer. CO_2 uptake at 1 atm ($p/p^0 = 0.0156$) and 298 K (25°C): 0.5 mmol.g^{-1} for the silica monolith and 2.2 mmol.g^{-1} for the carbon monolith.

S7- Comparison of catalytic activity with literature

Table S.2. Comparison of catalytic activity with literature

| Catalyst	Remarks	T (°C)	P (atm)	TON	TOF (min^{-1})	Ref
Homogeneous catalysis						
*Me*FoDH1	*Batch reactor – free enzymes*	**25**	**1**	**4 460**	**149**	**Our study**
*Cb*FoDH	Electrochemical regeneration w/o NAD (Artificial cofactor)	25	1	16	16	[7]
Ir complex	Pincer complex	140	80 H_2/CO_2	3 500 000	1 217	[8]
Ru complex	[$Ru_3(CO)_{12}$] in Ionic liquid	80	60 H_2/CO_2	17 000	5	[9]
Supported catalysis						
*Me*FoDH1	*Flow reactor - CLEAs@Carbon*	**25**	**1**	**6 653**	**166**	**Our study**
*Cb*FoDH	*Cb*FoDH@Rh-NU-1006 (MOF) Photochemical NAD regeneration	RT	1	346[†]	14[†]	[10]
*Cb*FoDH	*Cb*FoDH@Core-shell NP No NAD regeneration	37	1	15	0.25	[11]
Ru complex	Ru@Covalent triazine framework	120	80 H_2/CO_2	20 000	646[§]	[12]
Ir complex	Ir@Porous organic polymer	140	80 H_2/CO_2	25 135	18[‡]	[13]
Ir complex	Ir-PEI@Titanate nanotube	140	20 H_2/CO_2	1 012	129	[14]
PdAg NP	PdAg@SBA-15	100	20 H_2/CO_2	874	0.6	[15]
Ru complex	Ru@bpyTN-30-CTF Fixed bed continuous flow reactor	140	140 H_2/CO_2	524 000[¥]	12[¥]	[16]
*Dv*H-FoDH	Gas diffusion electrode w/o NAD (Viologen mediator)	RT	1	2 460[Ŧ] (66 243)[$]	0.9[Ŧ] (23)[$]	[17]
Sn NP	Electrocatalysis – flow cell	70	1	184[‖]	1[‖]	[18]
2D-Bi	Electrocatalysis – flow cell	RT	1	35 000[Σ]	20	[19]
*Dv*H-FoDH	RuP|TiO_2|*Dv*H-FoDH Photocatalysis w/o NAD	25	1	485 000[£]	660[¤]	[20]
Sn-GaN-Si	Photoelectrocatalysis (at - 0.53 V *vs.* RHE)	RT	1	64 000[#]	107[#]	[21]
Sn-GaN-Si	Photocatalysis (at + 0.02 V *vs.* RHE)	RT	1	312[¶]	2.6[¶]	[21]

[†]Determined over 24 hours; [§]Determined in the first 15 minutes; [‡]over 20 hours; [¥]over 30 days; [Ŧ]over 48 hours at - 0.59 V *vs.* SHE, according to HPLC analysis; [$]over 48 hours at - 0.59 V *vs.* SHE, based on the current density and assuming a faradaic efficiency (FE) of 100 %; [‖]Calculated from a partial current density of 51.7 mA cm^{-2} and a FE of 93.3 % over 3 hours; [Σ]Calculated from a partial current

density of 30 mA cm^{-2} and an average FE of 80 % over 100 hours; $^{£}$over 24 hours; $^{¤}$over 6 hours; $^{#}$over 10 hours; ¶over 2 hours.

References

[1] T. W. Johannes *et al.* Directed evolution of a thermostable phosphate dehydrogenase for NAD(P)H regeneration, *Appl. Environ. Microbiol. 71*, **2005**, 5728-5734

[2] R. Cazelles *et al.* Reduction of CO_2 to methanol by a polyenzymatic system encapsulated in phospholipids-silica nanocapsules. *New J. Chem. 37*, **2013**, 3721-3730.

[3] H. Choe *et al.* Efficient CO_2-reducing activity of NAD-dependent formate dehydrogenase from *Thiobacillus sp.* KNK65MA for formate production from CO_2 gas, *PLOS ONE 9*, **2014**, e103111

[4] K. Sakai *et al.* Interconversion between formate and hydrogen carbonate by tungsten-containing formate dehydrogenase-catalyzed mediated bioelectrocatalysis, *Sens. Bio-sensing Res. 5*, **2015**, 90-96

[5] K. Szymanska *et al.*, Low back-pressure hierarchically structured multichannel microfluidic bioreactors for rapid protein digestion – Proof of concept, *Chem. Eng. J. 287*, **2016**, 148-154

[6] L. Yu *et al.* Hydrothermal nanocasting : synthesis of hierarchically porous carbon monoliths and their application in lithium-sulfur batteries, *Carbon 61*, **2013**, 245-253

[7] S. Ikeyama *et al.* An artificial co-enzyme based on the viologen skeleton for highly efficient CO_2 reduction to formic acid with formate dehydrogenase, *ChemCatChem 9*, **2017**, 833-838

[8] R. Tanaka *et al.* Catalytic Hydrogenation of Carbon Dioxide Using Ir(III)-Pincer Complexes, *J. Am. Chem. Soc. 131*, **2009**, 14168–14169

[9] A. Weilhard *et al.* Selective CO_2 Hydrogenation to Formic Acid with Multifunctional Ionic Liquids, *ACS Catal. 8*, **2018**, 1628-1634

[10] Y. Chen *et al.* Integration of Enzymes and Photosensitizers in a Hierarchical Mesoporous Metal–Organic Framework for Light-Driven CO_2 Reduction, *J. Am. Chem. Soc. 142*, **2020**, 1768-1773

[11] Y.K. Kim *et al.* Enhancement of formic acid production from CO_2 in formate dehydrogenase reaction using nanoparticles, *RSC Adv. 6*, **2016**, 109978- 109982

[12] G. H. Gunasekar *et al.* Hydrogenation of CO_2 to Formate using a Simple, Recyclable, and Efficient Heterogeneous Catalyst, *Inorg. Chem. 58*, **2019**, 3717−3723

[13] X. Shao *et al.* Iridium single-atom catalyst performing a quasi-homogeneous hydrogenation transformation of CO_2 to formate, *Chem. 5*, **2019**, 693–705.

[14] Y. Kuwahara *et al.*,Poly(ethyleneimine)-tethered Ir complex catalyst immobilized in titanate nanotubes for hydrogenation of CO_2 to formic acid, *ChemCatChem 9*, **2017**, 1906-1914.

[15] K. Mori *et al.* Phenylamine-functionalized mesoporous silica supported PdAg nanoparticle: a dual heterogeneous catalyst for the formic acid/CO_2-mediated chemical hydrogen delivery/storage, *Chem. Commun. 53*, **2017**, 4677-4680.

[16] K. Park *et al.* CO_2 hydrogenation to formic acid over heterogenized ruthenium catalysts using a fixed bed reactor with separation units, *Green Chem. 22*, **2020**, 1639-1649.

[17] J. Szczesny *et al.* Electroenzymatic CO_2 Fixation Using Redox Polymer/Enzyme-Modified Gas Diffusion Electrodes, *ACS Energy Lett. 5*, **2020**, 321-327.

[18] W. Lee *et al.* Catholyte-Free Electrocatalytic CO_2 Reduction to Formate, *Angew. Chem. Int. Ed. 57,* **2018**, 6883-6887.

[19] C. Xia *et al.* Continuous production of pure liquid fuel solutions via electrocatalytic CO_2 reduction using solid-electrolyte devices, *Nature Energy 4,* **2019**, 776-785.

[20] M. Miller *et al.* Interfacing Formate Dehydrogenase with Metal Oxides for the Reversible Electrocatalysis and Solar-Driven Reduction of Carbon Dioxide, *Angew. Chem. Int. Ed. 58,* **2019**, 4601-4605.

[21] B. Zhou *et al.* A GaN:Sn nanoarchitecture integrated on a silicon platform for converting CO_2 to HCOOH by photoelectrocatalysis, *Energy Environ. Sci. 12,* **2019**, 2842-2848.